



Copyright © 2011 American Scientific Publishers
All rights reserved
Printed in the United States of America

Journal of
Nanoscience and Nanotechnology
Vol. 11, 1–9, 2011

Emission Modulation of DNA-Templated Fluorescent Silver Nanoclusters by Divalent Magnesium Ion

Kun Ma, Qinghua Cui, Yong Shao*, Fei Wu, Shujuan Xu, and Guiying Liu

Institute of Physical Chemistry, Zhejiang Normal University, Jinhua 321004, Zhejiang, People's Republic of China

DNA-templated fluorescent silver nanoclusters (Ag NCs) composed of several or tens of atoms are gaining much interest because of their unique properties and convenient emission tunability by DNA sequence and length. However, the modulation by other factors other than DNA is also dependent on the special DNA secondary structure formation such as *i*-motif or G-quadruplex that is stimulated by pH or K⁺. One main observation considered in this work is emission modulation of Ag NCs by divalent Mg²⁺ during or after the clusters' creation. Tuning the emitting intensities and band positions can be realized by Mg²⁺ addition for the examined single-stranded DNA (ss-DNA) templates, which is dependent on the addition moment of Mg²⁺, while only intensity modulation should be achieved for the used double-stranded DNA (ds-DNA). Despite of this discrepancy, Mg²⁺ addition always induces a lifetime-varied emission state of Ag NCs. The modulated emission still follows the common nature of the previously used DNA sequence- and length-dependent emitting. Efficient screening the negative charges of DNA backbone upon addition of the divalent ion is responsible for the modulation by adaptively accommodating the formed Ag NCs. This strategy could be more advantageous over the emission modulation by DNA sequence and length because a desired emitting could be achieved only by alteration of the electrolyte conditions during or after the Ag NCs' creation.

Keywords:

1. INTRODUCTION

Silver nanoclusters (Ag NCs) as an emerging set of fluorophores have attracted much attention because of their unique properties such as brightness, photostability and subnanometer size which could find wide applications in the field of sensing, catalysis, surface-enhanced Raman scattering (SERS).^{1–6} In order to stabilize the Ag NCs during the synthesis process and further applications, many efforts have been made to synthesize fluorescent Ag NCs by using varieties of capping scaffolds^{7,8} such as chitosan, ionic liquid, dendrimer and polymers.^{9–14} Interestingly, biomolecules such as peptide,^{15–17} protein^{18–20} have also been employed as alternative biotemplates for biocompatibility consideration. Followed by Dickson's work²¹ and on the basis of the fact that Ag⁺ favors specific binding mainly to DNA's heterocyclic bases rather than to its phosphate backbone,^{22,23} nucleic acids (DNA) have been widely accepted as novel biocompatible scaffolds because of the convenience in DNA chemical synthesis for variable DNA sequence and length. Among them, oligonucleotidic

single-stranded DNAs (ss-DNAs) as capping scaffolds hold great potentials for synthesis of Ag NCs emitters with tunable emissions from blue to near-infrared regions^{21,24–51} and variable quantum yields up to 64%.³¹ For example, the ss-DNAs with same 12-mer length and base composition but variable base combinations (5'-CCCTCTTAACCC-3', 5'-CCCTTTAACCCC-3', and 5'-CCCTTAATCCCC-3') have been used to create highly fluorescent blue, green, and yellow emitters.²⁶ 5'-TATCCGT-C_n-ACGGATA-3' hairpin can produce Ag NCs with emissions from 525 to 686 nm by varying the loop *n* between 3 and 12.³⁸ However, pure water^{26,28,31,37,50} and buffered salt conditions^{21,26–35,39,42,44–51} were used to produce these Ag NCs and the roles of them were not very clear. Additionally, double-stranded DNAs (ds-DNA) with functional segments such as polycytosine bulge,⁵² mismatch⁵³ or abasic site⁵⁴ have been occasionally demonstrated to accommodate fluorescent Ag NCs, of course in buffered conditions, and used for *in situ* single-nucleotide polymorphism (SNP) DNA biosensing at the same time of their synthesis. In the field of post-synthetic applications, ss-DNAs have attracted much attention due to the successful applications in cell biolabeling^{37,42,51} and chemical or biological

* Author to whom correspondence should be addressed.

sensing such as toxic metal ions^{32, 33, 43} and biothiols.^{39, 40} During these processes, the coexisted species with the analytes of interest in the tested samples would affect the fluorescence performance of formed Ag NCs by competitively binding the ss-DNAs bases or directly approaching the surface of Ag NCs. It has been confirmed that solution pH has effects on the formation of Ag NCs using ss-DNAs as capping scaffolds by pH-induced i-motif formation,^{27, 30} protonation and deprotonation of cytosine for Ag NCs binding sites in DNA.⁴⁰ Recently, K⁺-induced G-quadruplex conversion can also tune the emission of the templated Ag NCs for DNA logic device operation.³⁵ However, these modulations are DNA structure specific. In addition, excess of bivalent Mg²⁺ in a sample (for example blood serum) would bring a profound effect on the detection of trace quantity of analytes such as heavy metal ions Cu²⁺,^{32, 33} Hg²⁺,⁴³ and biothiols.^{39, 40} Therefore, elucidating the effect of non-specific bivalent Mg²⁺ on the fluorescence of Ag NCs is very important for Ag NCs synthesis and practical applications.^{7, 21, 24, 26, 28, 34, 44, 45, 52} In this work, silver nanoclusters templated by 5'-CGCTGCCCCCACCAT-3' and previously reported ss-DNAs were synthesized, and the influence of Mg²⁺ on the fluorescence of Ag NCs was investigated through varying their concentrations and changing the order of its addition. It is interesting to find out that the generation of fluorescent Ag NCs templated by ss-DNA was very sensitive to Mg²⁺ additions by observations of changes in both emission intensity and position. However, Ag NCs produced by a ds-DNA containing an abasic site or a mismatched base pair experience an increase in fluorescence intensity upon addition of Mg²⁺ instead with the emission position unchangeable. It is the first time to report that Mg²⁺ can generate distinct modulation on Ag NCs emission. Because of Mg²⁺ binding mainly at DNA phosphate backbone,²² this modulation could be explained by redistribution of the flexible structure of ss-DNAs on silver NCs surface after neutralizing the negative charge by Mg²⁺.

2. EXPERIMENTAL DETAILS

DNA strands were synthesized by TaKaRa Biotechnology Co., Ltd. (Dalian, China). All DNA samples were purified by HPLC. Other reagents were of analytical grade and used without purification. The DNA concentrations in single-stranded format were measured at 260 nm in pure water on the basis of extinction coefficients calculated by the nearest neighbor analysis.⁵⁵ AgNO₃ (Sigma-Aldrich Ltd.) with or without phosphate buffer (pH = 7.0) and magnesium acetate was added to the ss-DNA solution (5 μM if not stated) to an appropriate molar ratio. After mixing, the solution was incubated for 15 minutes with gentle stirring. It was then reduced by fast addition of freshly prepared NaBH₄ to an appropriate quantity as required and allowed to react for up to

DNA1-Y: 5'-CGCTGCCYCCACCAT-3'

Y = C, A, G, or T

DNA2: 5'-CCCTCTTAACCC-3'

DNA3: 5'-CCCTTAATCCCC-3'

DNA4: 5'-GCTCATGGTGGAGGCAGCGCCTC-3'
3'-CGAGTACCACCCCGTCGCGGAG-5'

DNA5: 5'-ATGGTGGXGGCAGCG-3'
3'-TACCACCCCGTCGC-5'

X = Abasic site

Scheme 1. The examined sequences of ss-DNAs (DNA1, DNA2, and DNA3) and ds-DNAs (DNA4 and DNA5).

4 h at 4 °C. The resulting solutions were examined at room temperature within 2 h. The Ag NCs templated by DNA2 and DNA3 (Scheme 1) were synthesized according to the previous procedure²⁶ with 1:6:6 molar ratios of DNA:Ag⁺:NaBH₄. To prepare DNA duplex solutions (mismatched DNA for DNA4 and abasic site-containing DNA for DNA5), the two strands were mixed in equimolar amounts and annealed in a thermocycler (first at 92 °C, then cooled down to room temperature slowly) in 20 mM phosphate buffer (pH 7.0). Tetrahydrofuran residual was used as the chemically stable abasic site for replacement of naturally tautomeric deoxyribose aldehyde structure. Nanopure water (18.2 mΩ; Millipore Co., USA) was used in all experiments. Fluorescence spectra were acquired with a FLSP920 spectrofluorometer (Edinburgh Instruments Ltd., UK) at 18 ± 1 °C, equipped with a temperature-controlled circulator (Julabo, Germany). Time-resolved fluorescence decays were recorded on a time-correlated single photon counting FLSP920 system, with excitation at less than 400 nm. A Ludox solution was used as scatter for the instrument response. The data were fitted with a multiexponential decay and χ² was less than 1.2. UV/Vis absorption spectra and were determined with a UV2550 spectrophotometer (Shimadzu Corp., Japan), equipped with an accessory of TMSPC-8 system which can simultaneously control the chamber temperature and detect up to 8 samples by a micro multi-cell. Sizes of the concomitantly formed large silver nanostructures were acquired with a JEOL 2010F transmission electron microscope (TEM). TEM samples were prepared by dropping a dispersion of Ag NCs onto a Cu grid covered by a holey carbon film.

3. RESULTS AND DISCUSSION

3.1. Emission Modulation of DNA-templated Ag NCs

Fluorescent Ag NCs were first formed using DNAs as capping scaffolds. For a general consideration, the used

DNA1 sequences are not self-complementary or hairpined and avoided to produce complex secondary DNA structures. In an optimized experiment, 5 μ M DNA1 was mixed with AgNO_3 solution (AgNO_3/DNA concentration ratio of 10:1) at the desired medium. The resultant solution was incubated for 15 minutes under stirring and then reduced by fast addition of NaBH_4 ($\text{NaBH}_4/\text{Ag}^+$ concentration ratio of 0.9:1) and left to react for 4 h to produce Ag NCs. As shown in Figure 1(A), DNA1-C produced at water provides the excellent template for the fluorescent clusters with emissions peaked at 508 nm by excitation

at 436 nm. However, substitution of A, G, or T for C in the very middle of DNA1 to give DNA1-A, DNA1-G, or DNA1-T dramatically decreases the intensities. However, addition of phosphate buffer (pH 7.0) alone or Mg^{2+} alone or both of them during the synthesis to DNA1-C solution totally quenches the emission with unnoticeable changes for other DNA1s. Interestingly, a new long-wavelength emission band peaked at 640 nm for DNA1-C appears with excitation at 560 nm, which is actually distinct only in the presence of Mg^{2+} by comparison with the cases for buffer alone, Mg^{2+} alone, and buffer plus Mg^{2+} , while

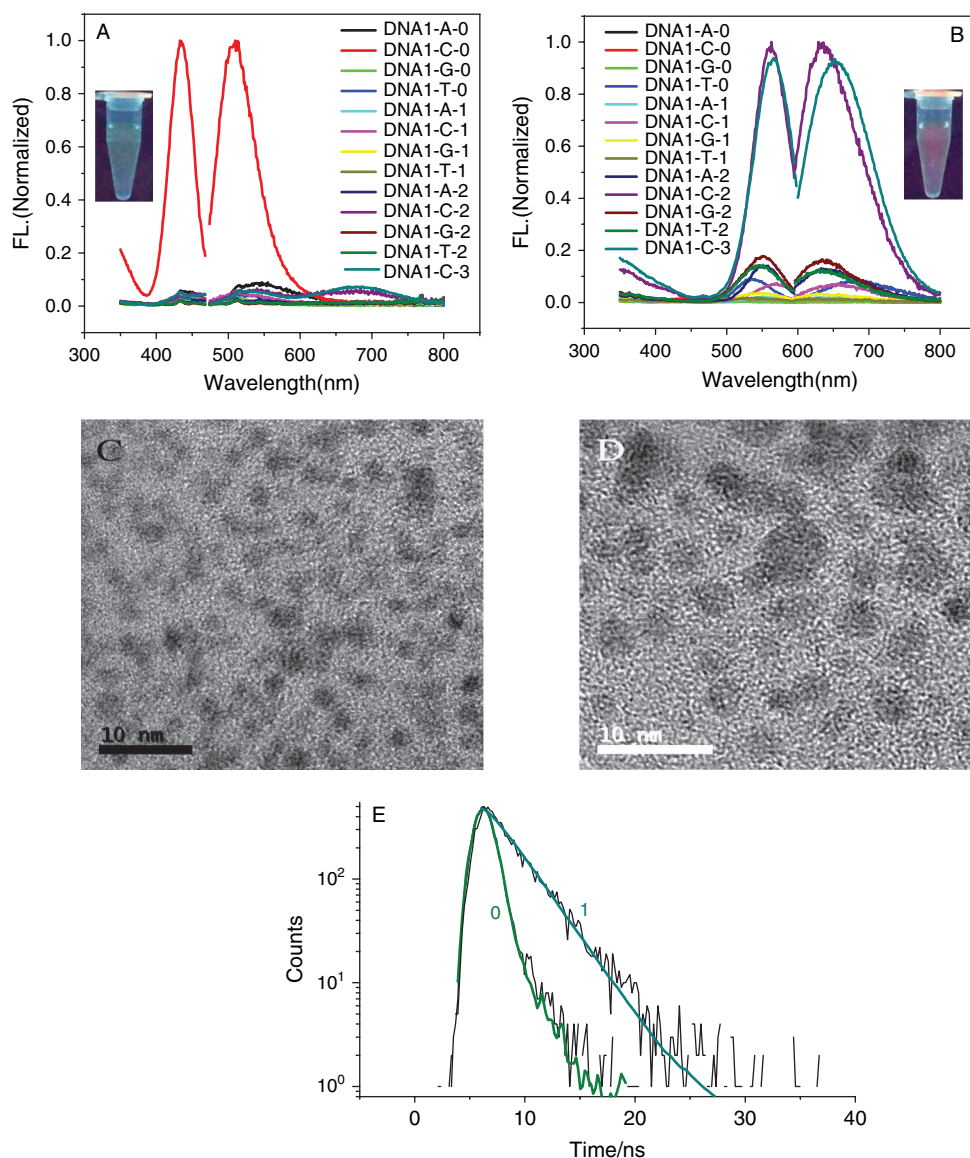


Fig. 1. (A and B) Fluorescence excitation and emission spectra of Ag NCs with DNA1-Ys (Y = A, C, G, T) as capping scaffolds. The Ag NCs were synthesized in (0) pure water, (1) 5 mM phosphate buffer (pH = 7.0), (2) 5 mM phosphate buffer (pH=7.0) and 1 mM Mg^{2+} , or (3) 1 mM Mg^{2+} . The small variations in excitation and emission wavelengths for Mg^{2+} alone result from pH changes caused by magnesium acetate addition. Inset: photographs of the fluorescent Ag NCs (templated by DNA1-C) generated at the conditions of 0 and 2 under UV illumination. TEM images of DNA1-C-templated Ag clusters synthesized in pure water (C) or phosphate buffer (pH = 7.0) containing Mg^{2+} (D) were given. (E) Time-resolved emission decays of Ag NCs templated by DNA1-C without (0) and with (1) addition of phosphate buffer and Mg^{2+} . The samples were irradiated by 335 nm, 40 MHz hydrogen-filled flash lamp.

Mg²⁺ addition induces or increases the emissions almost at the same wavelengths for replacement of C by A, G, or T at the same position in DNA1-C but with relative small variations in intensities relative to DNA1-C. The average sizes of these nanosilvers revealed by TEM images are about 1.9 nm and 2.8 nm synthesized in pure water and Mg²⁺-containing phosphate buffer (pH = 7.0), respectively (Figs. 1(C and D)). The almost similar maxima in the excitation and emission spectra of the long-wavelength bands for all DNA1-Ys indicate that the emission emitters result from the same electronic transition in the presence of Mg²⁺, not dependent on the DNA1 sequences although with different intensities. Such large shifts in emission wavelengths modulated by Mg²⁺ have not been achieved by other chemical stimuli like pH^{27, 30, 35, 40} and K⁺.³⁵ Additionally, the Ag NCs' emission exhibits single-exponential decay kinetics with fluorescence lifetime measurement by fitting (Fig. 1(E)) for synthesizing either in water (0.24 ns) or in Mg²⁺-containing phosphate buffer (2.68 ns), indicating only one dominant species presents for either case and emission modulation from 508 nm to 640 nm is entirely converted. These almost totally off- and on- switch in the short and long wavelengths by Mg²⁺ stimulus is very advantageous for such applications as DNA logic device construction.³⁵ As shown in Figure 2, relative to the phosphate buffer concentrations, the modulation is sharply dependent on Mg²⁺ concentrations in which 1 mM is more effective.

Ag NCs' emission is usually affected by their creation conditions. Addition manner of phosphate buffer and Mg²⁺ was also investigated here. As shown in Figure 3, the strongest emission is observed when Ag NCs' synthesis was carried out in phosphate buffer and Mg²⁺ solution, which is followed by the synthesis in the presence of Mg²⁺ but with post-synthetic addition of 5 mM phosphate buffer. However, a little weak fluorescence response is achieved in phosphate buffer during the synthesis and with Mg²⁺ post-synthetic addition, but still overrun the case of pure-water creation first and then with Mg²⁺-containing phosphate buffer added after completion of the synthesis. All these results suggest that Mg²⁺ addition during the synthesis creates more effective emissions than its post-synthetic addition, but this influence is weakened when adding Mg²⁺ ions to the system after the formation of Ag NCs.

To demonstrate generality of the modulation in Ag NCs' emission by Mg²⁺, we extended this approach to DNA2 (Fig. 4) and DNA3 (Fig. 5). DNA2 and DNA3 have been used to synthesis Ag emitters with efficient modulation in emissions.²⁶ Here 50 μM DNA2 was employed with 1:6:6 concentration ratios of DNA:Ag⁺:NaBH₄ and Ag NCs templated by DNA2 was initially synthesized in pure water. As shown in Figure 4(A), addition of phosphate buffer into the Ag NCs solution preformed in pure water sharply decreases the emission at 660 nm

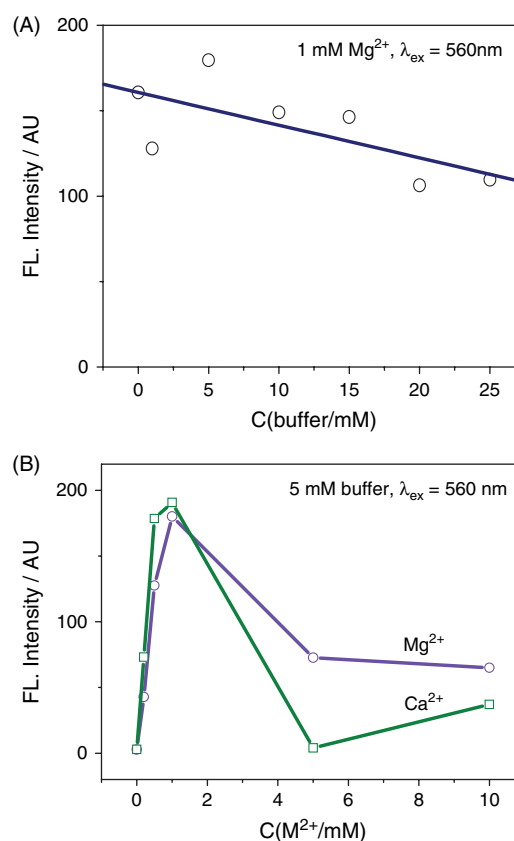


Fig. 2. (A) Dependences of the fluorescence intensities for DNA1-C at 640 nm on the phosphate buffer concentrations in the presence of 1 mM Mg²⁺ (A) and on Mg²⁺ or Ca²⁺ concentrations (B) in the presence of 5 mM phosphate buffer during the synthesis of Ag NCs.

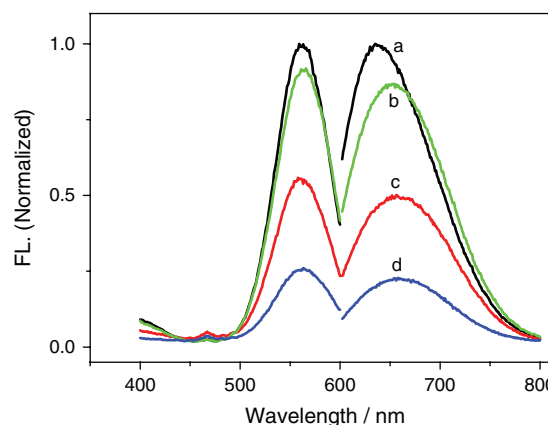


Fig. 3. Fluorescence excitation and emission profiles ($\lambda_{\text{ex}} = 560$ nm, $\lambda_{\text{em}} = 640$ nm) of Ag NCs templated by DNA1-C in different experimental conditions: (a) Ag NCs synthesis in 5 mM phosphate buffer and 1 mM Mg²⁺; (b) Ag NCs synthesis in 1 mM Mg²⁺ with post-synthetic addition of 5 mM phosphate buffer; (c) Ag NCs synthesis in 5 mM phosphate buffer with post-synthetic addition of 1 mM Mg²⁺; (d) Ag NCs synthesis in pure water with post-synthetic addition of 5 mM phosphate buffer and 1 mM Mg²⁺.

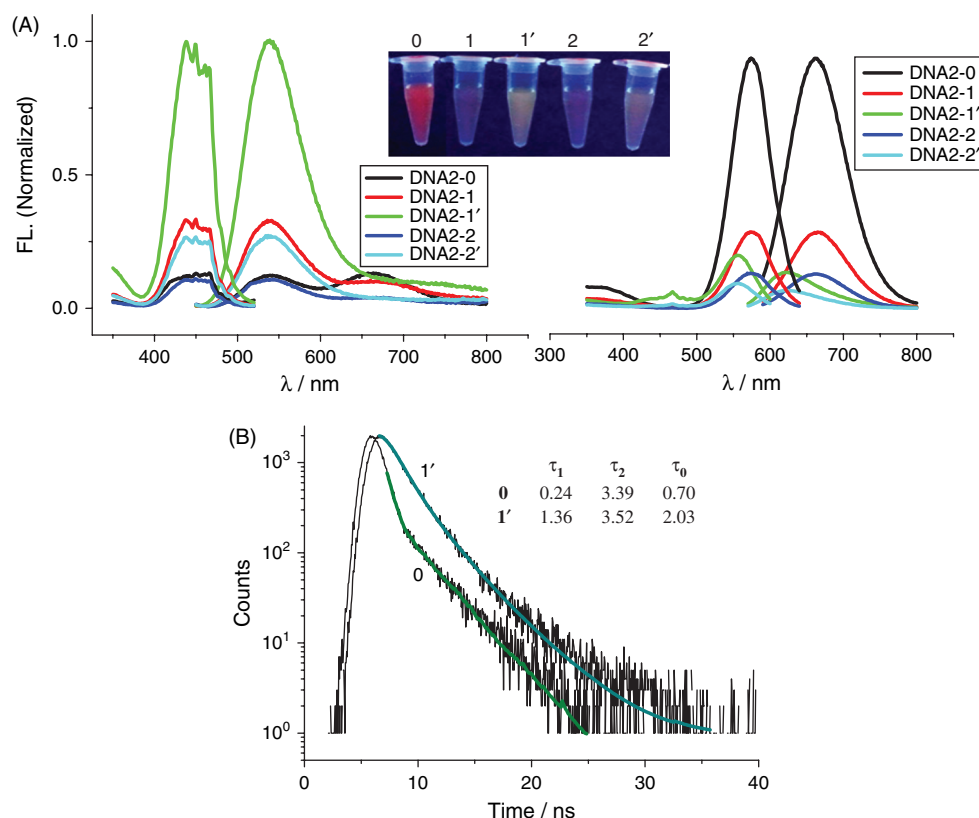


Fig. 4. (A) Fluorescence excitation and emission spectra of Ag NCs with DNA2 as capping scaffolds in different experimental conditions: (0) Ag NCs synthesis in pure water, (1) Ag NCs synthesis in pure water with post-synthetic addition of 5 mM phosphate buffer (pH = 7.0); (1') Ag NCs synthesis in pure water with post-synthetic addition of 5 mM phosphate buffer (pH = 7.0) and 1 mM Mg^{2+} ; (2) Ag NCs synthesis in 5 mM phosphate buffer (pH = 7.0); (2') Ag NCs synthesis in 5 mM phosphate buffer (pH = 7.0) with post-synthetic addition of 1 mM Mg^{2+} . Inset: photographs of the fluorescent Ag NCs generated at different conditions under UV illumination. (B) Time-resolved emission decays of Ag NCs templated by DNA2 without (0) and with (1') addition of phosphate buffer and Mg^{2+} . The samples were irradiated by 350 nm, 40 MHz hydrogen-filled flash lamp. Inset: the corresponding fluorescence time-resolved (τ_1 , τ_2) and average (τ_0) lifetimes (ns).

(excited at 574 nm) and increases the emission at 538 nm (excited at 438 nm). This modulation in intensities is much more significant upon addition of Mg^{2+} -containing phosphate buffer, accompanied by a blue shift for the long-wavelength emission band to 622 nm (excited at 556 nm). The similar modulations in emission bands are also observed for the Ag NCs preformed in phosphate buffer. The fluorescence difference after buffer and Mg^{2+} modulation is readily distinguishable by naked eye under UV illumination (Inset of Fig. 4(A)). The clusters templated by DNA2 exhibit biexponential decay kinetics behavior with an average lifetime of 0.70 ns in water and a prolonged average lifetime 2.03 ns at Mg^{2+} -containing phosphate buffer (Fig. 4(B)). On the basis of the amplitudes from the fits, the less stable species (0.24 ns) in water represent 85% of the total population of the clusters have a decay rate that is 14 times slower than that of the minor species (3.39 ns). However, after modulated by Mg^{2+} , the major fraction (1.36 ns) with a contribution of 69% has a decay rate that is only 2.6 times slower than that of the long-lived species (3.52 ns), indicating that Mg^{2+} addition can tune the emissions at the two wavelengths.

The emission of the Ag NCs templated by DNA3 (synthesized in 50 μM DNA3 with 1:6:1.2 concentration ratios of DNA: Ag^+ : $NaBH_4$) is also tuned by observations of Mg^{2+} -induced more sharp intensity increases and decreases in the short and long wavelength regions than the buffer alone (Fig. 5(A)). However, the red emitters are still abundant (Inset of Fig. 5(A)) and the emission lifetime is decreased (Fig. 5(B)) after Mg^{2+} additions. The Ag NCs templated by DNA3 have been used to DNA hybridization,²⁹ aptamer for thrombin⁴⁸ and probe for Cu^{2+} detection.³² As shown in Figure 5(C), the presence of Mg^{2+} significantly decreases the sensitivity for Cu^{2+} response by monitoring the emissions in short wavelength regions.

Previously, double-stranded DNAs (ds-DNA) with special functional segments such as mismatched base pair⁵³ and abasic site⁵⁴ were developed to be served as the growth spots for Ag NCs and biosensing applications. Here the modulation by Mg^{2+} is also applied to these ds-DNAs. As shown in Figure 6(A), the Ag NCs templated by DNA4 which contains a mismatched base pair experiences enhancement of the emission intensity upon Mg^{2+} addition

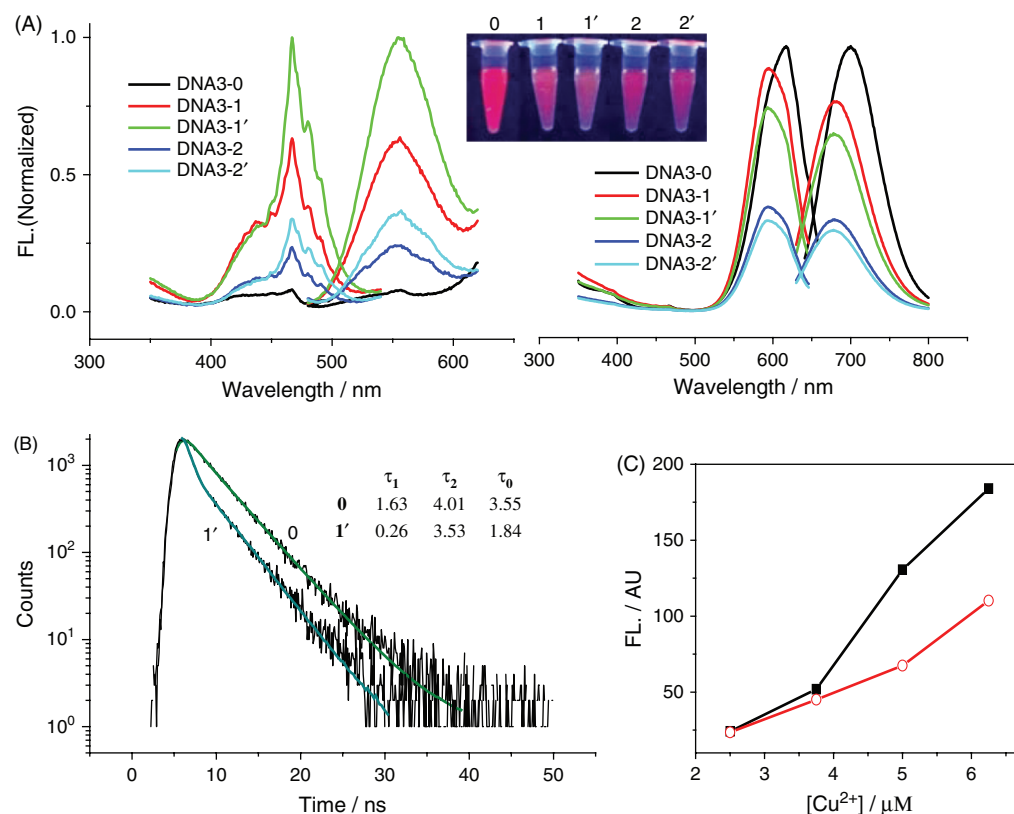


Fig. 5. (A) Fluorescence excitation and emission spectra of Ag NCs with DNA3 as capping scaffolds in different experimental conditions: (0) Ag NCs synthesis in pure water, (1) Ag NCs synthesis in pure water with post-synthetic addition of 5 mM phosphate buffer (pH = 7.0); (1') Ag NCs synthesis in pure water with post-synthetic addition of 5 mM phosphate buffer (pH = 7.0) and 1 mM Mg^{2+} ; (2) Ag NCs synthesis in 5 mM phosphate buffer (pH = 7.0); (2') Ag NCs synthesis in 5 mM phosphate buffer (pH = 7.0) with post-synthetic addition of 1 mM Mg^{2+} . Inset: photographs of the fluorescent Ag NCs generated at different conditions under UV illumination. (B) Time-resolved emission decays of Ag NCs templated by DNA3 without (0) and with (1') addition of phosphate buffer and Mg^{2+} . The samples were irradiated by 350 nm, 40 MHz hydrogen-filled flash lamp. Inset: the corresponding fluorescence time-resolved (τ_1 , τ_2) and average (τ_0) lifetimes (ns). (C) The Cu^{2+} concentration-dependent emission intensities of DNA3-templated Ag NCs in the absence (square) and presence (circle) of 1 mM Mg^{2+} .

but with an almost invariable excitation and emission peak positions, as is opposite the Mg^{2+} -induced modulations of both for ss-DNA-templated Ag NCs. In addition, the presence of Mg^{2+} induces a long-lived emission state of the Ag NCs (Fig. 6(C)). The similar phenomenon is observed for DNA5 which contains an abasic site (Fig. 6(B)). This non-modulation in the emitting peak positions for the ds-DNA templates could be resulted from the rigid DNA structure, while the enhancements in intensities should be ascribed to the more thermal stabilities of the DNAs upon Mg^{2+} addition for better protecting the formed Ag NCs. For example, the melting temperatures (T_m) for 5 μM DNA4 in 20 mM phosphate buffer (pH 7.0) increased from 60.1 $^{\circ}\text{C}$ to 71.7 $^{\circ}\text{C}$ in the absence and presence of 1 mM Mg^{2+} .⁵⁶

3.2. Mechanism

It is well known that bivalent ions with high charge density such as Mg^{2+} and Ca^{2+} are more efficient to neutralize the negative charge in DNA phosphate diester backbone than monovalent ions like K^{+} and Na^{+} .^{57–59} Therefore, the DNA-encapsulated Ag NCs could be protected well in

the presence of Mg^{2+} or Ca^{2+} by decreasing the electrostatic repulsion along the DNA backbone. In order to prove this point, the Ag NCs' emission modulated by Mg^{2+} was compared with that by Ca^{2+} . From the results for DNA1-C in Figure 2(B), Ca^{2+} induces a more sharp increase for the modulated long-wavelength emission at the low concentration regions than Mg^{2+} , in agreement with the stronger DNA binding ability of Ca^{2+} than that for Mg^{2+} .⁵⁷ This point can be further strengthened by the observations that the modulation seems to be more efficient for divalent Mg^{2+} and Ca^{2+} than monovalent Na^{+} from the used buffer (Fig. 2). But at high concentrations of more than 1 mM, Ca^{2+} induces a more rapid decrease in the long-wavelength emission, maybe because more Ca^{2+} would make the DNA strand rigid enough to weaken its ability to effectively surround Ag NCs.

To further validate the role of the bivalent ions on the structure of ss-DNAs, absorption spectra were measured by comparison with the conditions that Ag^{+} was coexisted with the bivalent ions or not. Reduction by NaBH_4 was not performed for this motivation in order to avoid distur-

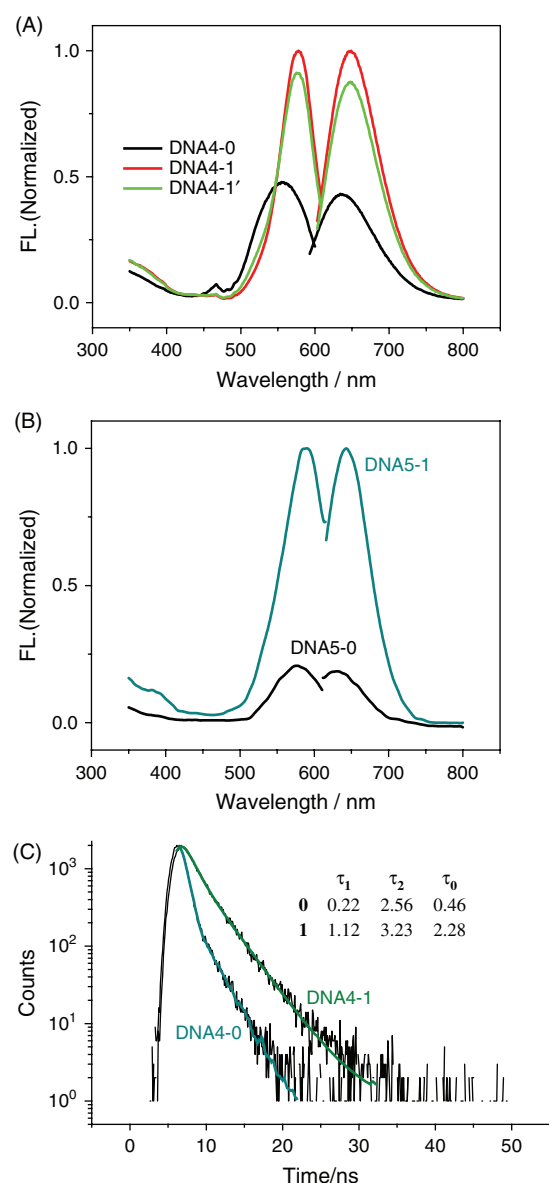


Fig. 6. Fluorescence excitation and emission spectra of Ag NCs with a mismatch-containing DNA (A, DNA4, ds-DNA) and an abasic site-containing DNA (B, DNA5, ds-DNA) as capping scaffolds in different experimental conditions: (0) Ag NCs synthesis in 20 mM phosphate buffer (pH = 7.0), (1) Ag NCs synthesis in 20 mM phosphate buffer (pH = 7.0) and 1 mM Mg^{2+} ; (1') Ag NCs synthesis in 20 mM phosphate buffer (pH = 7.0) with post-synthetic addition of 1 mM Mg^{2+} . (C) Time-resolved emission decays of Ag NCs templated by DNA4 without (0) and with (1) 1 mM Mg^{2+} . The samples were irradiated by 350 nm, 40 MHz hydrogen-filled flash lamp. Inset: the corresponding fluorescence time-resolved (τ_1 , τ_2) and average (τ_0) lifetimes (ns).

bance from the formed Ag NCs absorption. In addition, binding to heterocyclic DNA bases is kept for either Ag^{+60} or Ag clusters.⁶¹ As shown in Figure 7 with DNA1-C as a typical example, Mg^{2+} or Ca^{2+} alone induces a little decrease in absorption at 260 nm under room temperature by comparison with Ag^{+} alone, indicating the role of these bivalent ions by neutralizing the backbone

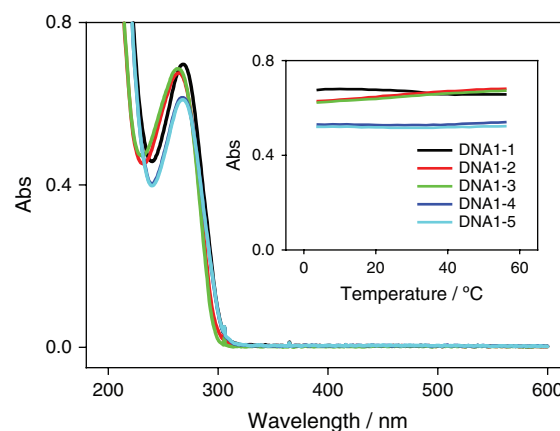


Fig. 7. UV-Vis absorption spectra and dependences of the 260 nm absorbance of 5 μM DNA1-C on temperatures (insert) in 5 mM phosphate buffer (pH 7.0) under different conditions: (1) Ag^{+} ; (2) Mg^{2+} ; (3) Ca^{2+} ; (4) $Ag^{+}+Mg^{2+}$; (5) $Ag^{+}+Ca^{2+}$. Ag^{+} : 50 μM ; Mg^{2+} and Ca^{2+} : 1 mM.

negative charge to result in a stronger base stacking. But this stability is weakened upon increasing temperature of the systems relative to the unchangeable absorption for Ag^{+} alone at the examined temperature regions, in agreement with Ag^{+} binding favorably and chemically to DNA heterocyclic bases and not phosphate backbone.^{22, 23} However, the coexistence of Mg^{2+} or Ca^{2+} with Ag^{+} induces a further decrease in the absorption and this gained stability is obvious enough to endure the temperature to be increased up to 60 $^{\circ}C$. These results prove that the presence of the bivalent ions makes the ss-DNA surround Ag^{+} more compactly and protect the lately formed NCs well from attacking by species in the solution. The fact that the presence of Mg^{2+} for DNA3-templated Ag NCs showed a less emission dependence on added Cu^{2+} at micromolar concentrations, relative to the case in the absence of Mg^{2+} (Fig. 5(C)), could be explained by this mechanism. The bivalent ions-induced base stacking to a high degree should also make the encapsulating DNA around the preformed Ag NCs redistribute on the cluster surface to achieve an emission modulation in position and intensity. Based on this model, the emission modulation can be easily achieved upon addition of the bivalent ions, even without variations in DNA sequences. Especially, the post-modulation after Ag NCs formation will make initiating a new synthesis event by another DNA template for a desired emission unnecessary (Figs. 3–5). This modulation should be more effective for ss-DNA template because of its flexible structure feature, relative to the rigid ds-DNA structure, which can be evidenced by the fact that modulation only in emission intensity occurred for DNA4 and DNA5 (Fig. 6), but further position modulation was realized for DNA1, DNA2, and DNA3 (Figs. 1, 4 and 5). It is expected that the size of Ag NCs has no chance to be changed upon Mg^{2+} post-addition for the preformed clusters (Figs. 3–5). Therefore, the Mg^{2+} -induced more packing between DNA bases

would make redistribution of ss-DNAs around the formed clusters so as to result in a new emission band because different binding site⁶² and interaction manner⁶³ between Ag NCs and the capsulate matrix would produce different electronic band structure. But for the rigid ds-DNA structure, this interaction rearrangement of DNA strand to the clusters couldn't occur, in agreement with the results for DNA4 and DNA5.

Another issue that should be concerned is whether the Mg^{2+} modulation in Ag NCs' optical properties is different from the other means or not. Although many efforts have been made to tune Ag NCs' emissions from blue to near-infrared regions by changing DNA sequences and lengths, these fascinating modulations in the dominant emissions seem follow a distinct trend. As shown in Figure 8, by grouping the data for the previously reported DNA-templated Ag NCs' optical properties, a linear dependence of the dominant emission energies (E_{em}) on excitation energies (E_{ex}), $E_{em} = (0.40 \pm 0.032) + (0.70 \pm 0.014) E_{ex}$ with a relative standard deviation 0.972, is mostly abided. Note that only dominant emission bands are collected from literatures and only several data^{26, 27} are against this relationship. This linear dependence means that about 70% of the excitation energies are effective for radiation transition from excited states to ground states after gaining a definite energy about 0.40 eV, indicating that modulation by any means should accord with this trend provided that DNA template is used, not very dependent on the size of Ag NCs, DNA sequence and length. Interestingly, the modulated emissions by Mg^{2+} in this work still follow this empirical tendency (Fig. 8), indicating the interplay between DNA bases and the clusters remains in the presence of Mg^{2+} . This linear dependence could be used to explain the possible mechanism of Ag NCs emission process that is regulated by the interaction of DNA bases with silver clusters.

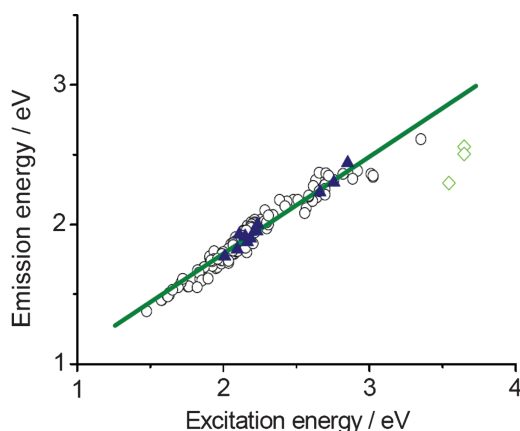


Fig. 8. The emission energies and corresponding excitation energies of fluorescent Ag NCs synthesised by DNA templates with a linear (circle) or out-of-linear (diamond) dependence. The data are derived from Refs. [21–51] for ss-DNAs and Refs. [52–54] for ds-DNAs. Our data in this work (triangle) are also agreed with this linear dependence.

4. CONCLUSION

In summary, emission modulation of fluorescent Ag NCs templated by DNA during or after the clusters' creation was achieved by divalent Mg^{2+} that has a nonspecific interaction with DNA backbone. Dependent on the addition moment of Mg^{2+} , the emitting intensities and band positions can be tuned for single-stranded DNA (ss-DNA) templates, while only intensity modulation should be achieved for double-stranded DNA (ds-DNA)-templated Ag NCs. In addition, Mg^{2+} addition always induces a lifetime-varied emission state of Ag NCs. The emission modulation is ascribed to efficient screening of the negative charges of DNA backbone upon addition of the divalent ion. This strategy provides the motivation to ascertain the factors that significantly influence the Ag NCs' emission by minor variations in the environments that surround the clusters.

Acknowledgments: This work was supported by the National Natural Science Foundation of China (Grant No. 21075112), the Qianjiang Talent Project from the Department of Science and Technology of Zhejiang Province (Grant No. 2009R10058), the Foundation of State Key Laboratory of Electroanalytical Chemistry, Changchun Institute of Applied Chemistry (Grant No. SKLEAC2010001) and the Scientific Research Foundation for Returning Overseas Chinese Scholars, State Education Ministry.

References and Notes

1. L. Shang and S. J. Dong, *J. Mater. Chem.* 18, 4636 (2008).
2. B. Adhikari and A. Banerjee, *Chem. Mater.* 22, 4364 (2010).
3. S. H. Liu, F. Lu, and J. J. Zhu, *Chem. Commun.* 47, 2661 (2011).
4. Y. Lei, F. Mehmood, S. Lee, J. Greeley, B. Lee, S. Seifert, R. E. Winans, J. W. Elam, R. J. Meyer, P. C. Redfern, D. Teschner, R. Schlögl, M. J. Pellin, L. A. Curtiss, and S. Vajda, *Science* 328, 224 (2010).
5. K. Esumi, R. Isono, and T. Yoshimura, *Langmuir* 20, 237 (2004).
6. L. Sun, Y. Sun, F. Xu, Y. Zhang, T. Yang, C. Guo, Z. Liu, and Z. Li, *Nanotechnology* 20, 125502 (2009).
7. H. Xu and K. S. Suslick, *Adv. Mater.* 22, 1078 (2010).
8. I. Díez and R. H. A. Ras, *Nanoscale* 3, 1963 (2011).
9. A. Murugadoss and A. Chattopadhyay, *Nanotechnology* 19, 015603 (2008).
10. H. J. Zhang, X. Y. Li, and G. H. Chen, *J. Mater. Chem.* 19, 8223 (2009).
11. J. Zheng and R. M. Dickson, *J. Am. Chem. Soc.* 124, 13982 (2002).
12. J. Zhang, S. Xu, and E. Kumacheva, *Adv. Mater.* 17, 2336 (2005).
13. L. Shang and S. Dong, *Chem. Commun.* 44, 1088 (2008).
14. S. K. Sun, H. F. Wang, and X. P. Yan, *Chem. Commun.* 47, 3817 (2011).
15. J. M. Slocik, J. T. Moore, and D. W. Wright, *Nano Lett.* 2, 169 (2002).
16. B. Adhikari and A. Banerjee, *Chem. Eur. J.* 16, 13698 (2010).
17. J. H. Yu, S. A. Patel, and R. M. Dickson, *Angew. Chem. Int. Ed.* 46, 2028 (2007).
18. N. Braun, W. Meining, U. Hars, M. Fischer, R. Ladenstein, R. Huber, A. Bacher, S. Weinkauff, and L. Bachmann, *J. Mol. Biol.* 321, 341 (2002).
19. S. S. Narayanan and S. K. Pal, *J. Phys. Chem. C* 112, 4874 (2008).

20. C. L. Guo and J. Irudayaraj, *Anal. Chem.* 83, 2883 (2011).
21. J. T. Petty, J. Zhang, N. V. Hud, and R. M. Dickson, *J. Am. Chem. Soc.* 126, 5207 (2004).
22. L. Berti and G. A. Burley, *Nat. Nanotechnol.* 3, 81 (2008).
23. H. Arakawa, J. F. Neault, and H. A. Tajmir-Riahi, *Biophys. J.* 81, 1580 (2001).
24. C. M. Ritchie, K. R. Johnsen, J. R. Kiser, Y. Antoku, R. M. Dickson, and J. T. Petty, *J. Phys. Chem. C* 111, 175 (2007).
25. S. Pal, R. Varghese, Z. T. Deng, Z. Zhao, A. Kumar, H. Yan, and Y. Liu, *Angew. Chem. Int. Ed.* 50, 4176 (2011).
26. C. I. Richards, S. Choi, J. C. Hsiang, Y. Antoku, T. Vosch, A. Bongiorno, Y. L. Tzeng, and R. M. Dickson, *J. Am. Chem. Soc.* 130, 5038 (2008).
27. B. Sengupta, C. M. Ritchie, J. G. Buckman, K. R. Johnsen, P. M. Goodwin, and J. T. Petty, *J. Phys. Chem. C* 112, 18776 (2008).
28. Y. Antoku, Ph.D. Thesis, Georgia Institute of Technology (2007).
29. H. C. Yeh, J. Sharma, J. J. Han, J. S. Martinez, and J. H. Werner, *Nano Lett.* 10, 3106 (2010).
30. B. Sengupta, K. Springer, J. G. Buckman, S. P. Story, O. H. Abe, Z. W. Hasan, Z. D. Prudowsky, S. E. Rudisill, N. N. Degtyareva, and J. T. Petty, *J. Phys. Chem. C* 113, 19518 (2009).
31. J. Sharma, H. C. Yeh, H. Yoo, J. H. Werner, and J. S. Martinez, *Chem. Commun.* 46, 3280 (2010).
32. G. Y. Lan, C. C. Huang, and H. T. Chang, *Chem. Commun.* 46, 1257 (2010).
33. Y. T. Su, G. Y. Lan, W. Y. Chen, and H. T. Chang, *Anal. Chem.* 82, 8566 (2010).
34. S. Choi, J. Yu, S. A. Patel, Y. L. Tzeng, and R. M. Dickson, *Photochem. Photobiol. Sci.* 10, 109 (2011).
35. T. Li, L. B. Zhang, J. Ai, S. J. Dong, and E. K. Wang, *ACS Nano* 5, 6334 (2011).
36. T. Driehorst, P. O'Neill, P. M. Goodwin, S. Pennathur, and D. K. Fygenson, *Langmuir* 27, 8923 (2011).
37. J. Yu, S. Choi, and R. M. Dickson, *Angew. Chem. Int. Ed.* 48, 318 (2009).
38. P. R. O'Neill, L. R. Velazquez, D. G. Dunn, E. G. Gwinn, and D. K. Fygenson, *J. Phys. Chem. C* 113, 4229 (2009).
39. Z. Z. Huang, F. Pu, Y. H. Lin, J. S. Ren, and X. G. Qu, *Chem. Commun.* 47, 3487 (2011).
40. B. Y. Han and E. K. Wang, *Biosens. Bioelectron.* 26, 2585 (2011).
41. G. Y. Lan, W. Y. Chen, and H. T. Chang, *Biosens. Bioelectron.* 26, 2431 (2011).
42. J. H. Yu, S. Choi, C. I. Richards, Y. Antoku, and R. M. Dickson, *Photochem. Photobiol.* 84, 1435 (2008).
43. W. W. Guo, J. P. Yuan, and E. K. Wang, *Chem. Commun.* 45, 3395 (2009).
44. E. G. Gwinn, P. O'Neill, A. J. Guerrero, D. Bouwmeester, and D. K. Fygenson, *Adv. Mater.* 20, 279 (2008).
45. Y. Fu, J. L. Zhang, X. F. Chen, T. T. Huang, X. L. Duan, W. Li, and J. K. Wang, *J. Phys. Chem. C* 115, 10370 (2011).
46. D. Schultz and E. Gwinn, *Chem. Commun.* 47, 4715 (2011).
47. T. Vosch, Y. Antoku, J. C. Hsiang, C. I. Richards, J. I. Gonzalez, and R. M. Dickson, *Proc. Natl. Acad. Sci. U.S.A.* 104, 12616 (2007).
48. J. Sharma, H. C. Yeh, H. Yoo, J. H. Werner, and J. S. Martinez, *Chem. Commun.* 47, 2294 (2011).
49. S. A. Patel, C. I. Richards, J. C. Hsiang, and R. M. Dickson, *J. Am. Chem. Soc.* 130, 11602 (2008).
50. S. A. Patel, M. Cozzuol, J. M. Hales, C. I. Richards, M. Sartin, J. C. Hsiang, T. Vosch, J. W. Perry, and R. M. Dickson, *J. Phys. Chem. C* 113, 20264 (2009).
51. Y. Antoku, J. I. Hotta, H. Mizuno, R. M. Dickson, J. Hofkens, and T. Vosch, *Photochem. Photobiol. Sci.* 9, 716 (2010).
52. W. W. Guo, J. P. Yuan, Q. Z. Dong, and E. K. Wang, *J. Am. Chem. Soc.* 132, 932 (2010).
53. Z. Z. Huang, F. Pu, D. Hu, C. Y. Wang, J. S. Ren, and X. G. Qu, *Chem. Eur. J.* 17, 3774 (2011).
54. K. Ma, Q. H. Cui, G. Y. Liu, F. Wu, S. J. Xu, and Y. Shao, *Nanotechnology* 22, 305502 (2011).
55. J. D. Puglisi and I. Jr. Tinoco, *Methods Enzymol.* 180, 304 (1989).
56. Melting temperatures were calculated based on Integrated DNA Technologies web site available at: <http://www.idtdna.com/analyzer/Applications/OligoAnalyzer/>.
57. N. Korolev, A. P. Lyubartsev, A. Rupprecht, and L. Nordenskiöld, *Biophys. J.* 77, 2736 (1999).
58. R. Owczarzy, B. G. Moreira, Y. You, M. A. Behlke, and J. A. Walder, *Biochemistry* 47, 5336 (2008).
59. Y. Bai, M. Greenfeld, K. J. Travers, V. B. Chu, J. Lipfert, S. Doniach, and D. Herschlag, *J. Am. Chem. Soc.* 129, 14981 (2007).
60. S. Shukla and M. Sastry, *Nanoscale* 1, 122 (2009).
61. V. Soto-Verdugo, H. Metiu, and E. Gwinn, *J. Chem. Phys.* 132, 195102 (2010).
62. M. Harb, F. Rabilloud, and D. Simon, *J. Phys. B: At. Mol. Opt. Phys.* 44, 035101 (2011).
63. I. Rabin, W. Schulze, G. Ertl, C. Felix, C. Sieber, W. Harbich, and J. Buttet, *Chem. Phys. Lett.* 320, 59 (2000).

Received: 29 August 2011. Accepted: 30 August 2011.